

# Molecularly Imprinted Polymers and Electrospinning: Manufacturing Convergence for Next-Level Applications

Kapil D. Patel, Hae-Won Kim, Jonathan C. Knowles, and Alessandro Poma\*

Micro- and especially nanofiber-type of materials are extremely attractive for a number of applications, ranging from separation and analysis to drug delivery and tissue engineering, and the majority of them are currently produced worldwide via the extremely popular and effective electrospinning technique. The addition of specific tailored molecular recognition capability to these electrospun materials via the established molecular imprinting technology can be extremely beneficial for a number of applications, as indicated by the number of examples in the literature over the past 15 years. However, the integration of these two technologies has proven to be quite challenging, mainly due to the different processing methodologies which characterize the two approaches. In this progress report, the practical difficulties related to the combination of electrospinning and molecular imprinting and to the production of molecularly imprinted electrospun fibers are addressed, discussing the main aspects to take into consideration when designing and optimizing the experimental protocols, as well as highlighting the most prolific research applications that have been explored thus far, to conclude with a commercial/industrial and economic perspective on the envisaged market for these hybrid products.

## 1. Electrospun Nanofibers: Attractive Manufacturing and Format

Nanotechnology and nanomaterials science are currently extremely attractive topics to be investigated for a plethora of applications, ranging from electronics to sensing/diagnostics to drug delivery and tissue engineering. The final format of the nanomaterials to be produced is normally strictly dependent on the ultimate usage, and indeed nanofiber-type materials have been increasingly utilized as membranes for purification

purposes in environmental engineering and biotechnology, for biological sensing in defense and security, as scaffolds for tissue engineering and regenerative medicine, and for energy applications such as solar and fuel cells.<sup>[1]</sup> This popularity derives from the intriguing characteristics of these nanomaterials, which include extremely high surface area to volume (due to the nanometer scale), but coupled with improved mechanical performance (e.g., tensile strength), high porosity and adjustable pore-size distribution, and ultimately versatility for the surface decoration with specific chemical moieties. This latter feature, together with the type of polymers used for the fabrication, can guarantee extremely high biocompatibility/biodegradability, essential in the case of healthcare and drug-delivery applications.<sup>[2]</sup>

The early history of fiber production dates back to 2700 B.C. for silk fibers and textiles, and since then tremendous technological advances have been made.<sup>[3]</sup> Nowadays, different methods can be used for nanofiber fabrication, such as bicomponent extrusion, template synthesis, self-assembly, phase separation, melt blowing, drawing, centrifugal spinning, and electrospinning.<sup>[4]</sup> Amongst these production methods, electrospinning is one of the most widely investigated and employed.

Electrospinning is a simple, versatile, cost-effective, and easily accessible technique for the production of micro-/nanofibers,<sup>[3a]</sup> with diameters ranging from tens of nanometers

Dr. K. D. Patel, Prof. H.-W. Kim  
Institute of Tissue Regeneration Engineering (ITREN)  
Dankook University  
Cheonan 31116, South Korea

Dr. K. D. Patel, Prof. H.-W. Kim, Prof. J. C. Knowles  
Department of Nanobiomedical Science and BK21 PLUS NBM Global  
Research Center for Regenerative Medicine Research Center  
Dankook University  
Cheonan 31116, South Korea

 The ORCID identification number(s) for the author(s) of this article can be found under <https://doi.org/10.1002/adfm.202001955>.

© 2020 The Authors. Published by WILEY-VCH Verlag GmbH & Co. KGaA, Weinheim. This is an open access article under the terms of the Creative Commons Attribution License, which permits use, distribution and reproduction in any medium, provided the original work is properly cited.

DOI: 10.1002/adfm.202001955

Dr. K. D. Patel, Prof. H.-W. Kim, Prof. J. C. Knowles  
UCL Eastman-Korea Dental Medicine Innovation Centre  
Dankook University  
Cheonan 31116, South Korea

Dr. K. D. Patel, Prof. J. C. Knowles, Dr. A. Poma  
Division of Biomaterials and Tissue Engineering  
UCL Eastman Dental Institute  
University College London  
256 Gray's Inn Road, London WC1X 8LD, UK  
E-mail: a.poma@ucl.ac.uk

Prof. H.-W. Kim  
Department of Biomaterials Science  
School of Dentistry  
Dankook University  
Cheonan 31116, South Korea

Prof. J. C. Knowles  
The Discoveries Centre for Regenerative and Precision Medicine  
UCL Campus, London, UK

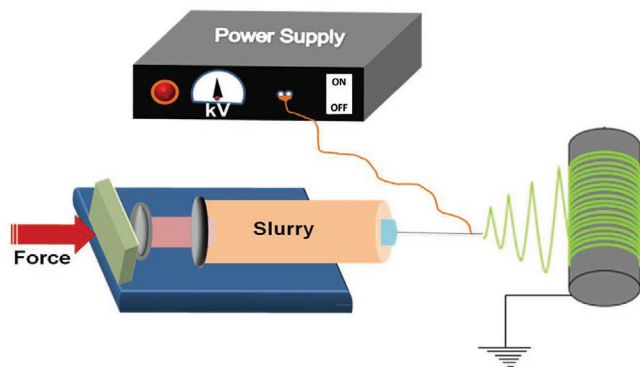


**Figure 1.** Schematic illustration of needle-based electrospinning set-up and production of fibers.

up to micrometers. Most of the synthetic and naturally occurring polymers can be electrospun following dissolution in appropriate solvents. In conventional spinning, shearing, rheological, gravitational, inertial, and aerodynamics forces act on the fibers. However, in electrospinning only electrostatic forces are employed to generate fibers,<sup>[5]</sup> based on the application of an electrical voltage to a polymer solution or melt.<sup>[6]</sup> A simple electrospinning setup is depicted in **Figure 1**, and it involves a syringe (solution container) end-tipped with a stainless steel or other conducting needle, a pump, a high-voltage power source, and a collector.

The polymer solution is pumped at a constant flow-rate and at a definite applied voltage and distance between the needle and the collector, resulting in the production of the desired materials. Depending on the electrospinning parameters, either fibers (nano- or micro-) or particles can be produced.<sup>[6]</sup>

The mechanism of electrospinning involves the accumulation of charges at the liquid surface due to the electrostatic repulsion caused by the electric field applied; once these electrostatic repulsion forces overcome the surface tension of the liquid, the meniscus is deformed into a conically shaped structure (Taylor cone).<sup>[7]</sup> This charged liquid jet is then ejected toward the collector (e.g., flat plates, rotating drums). Depending on the solution viscosity, solid fibers will be formed as the solvent evaporates from the whipping motion that occurs during the flight time from the cone shaped structure to the collector, thus ultimately resulting in the deposition of a non-woven fiber mat.

The effects of various processing parameters on the product morphology and performance have been extensively studied.<sup>[4,8]</sup> Some of these parameters (related to the solution, the setup and the environment) are more easily controllable, and will strongly influence the success of the process. To provide some examples, the electrical conductivity of the polymer solution (which depends on the type of polymer, solvent, and salt concentration) plays a vital role in controlling the fiber diameter size and distribution. A polymer solution with low electrical conductivity cannot produce fibers because the surface of the droplet does not carry enough electrical charge to form a Taylor cone. Conversely, polymer solutions with high electrical conductivity tend to produce small diameter fibers, up to a critical conductivity value above which the polymer solutions become extremely unstable and result in broad fiber-diameter divergence under



**Kapil D. Patel** received his M.Sc. in Physics from Indian Institute of Technology (IIT) Guwahati (2010) and Ph.D. in Tissue Regeneration Engineering from Dankook University, South Korea (2015), and continued as Postdoctoral Researcher (2016–2019) at the Institute of Tissue Regeneration Engineering (ITREN),

Dankook University. Currently, he is Research Professor at Dankook University and Visiting Research Fellow at University College London (UCL), UK. His research interests focused on the electrospinning nanofibers, functional nano-biomaterials for drug delivery, tissue repair and regeneration and cancer theranostics.



**Alessandro Poma** received his M.Sc. in Pharmaceutical Technology and Chemistry from the University of Palermo (Italy) in 2009. He then joined the Cranfield Biotechnology Group led by Prof. Sergey Piletsky to undertake a Ph.D. in Biosensors and Nanomaterials (Cranfield University, 2013). He moved to UCL in 2014, first as an

NC3Rs David Sainsbury Fellow and subsequently in other roles, and he has been recently appointed as Lecturer in Biomaterials and Allied Subjects in the Division of Biomaterials and Tissue Engineering. His key research area is the development of molecularly imprinted nanomaterials as synthetic antibodies, and their polymeric biodegradable composites for diagnostic, therapeutic, and tissue engineering applications.

the strong applied electrical field.<sup>[9]</sup> Other variables such as the distance of the collector from the needle could either result in no fiber deposition (if too long), or in possible arcing (if too short). Arcing can also take place if the applied voltage is too high, while too low voltage will not produce fibers because the electrostatic repulsion forces will be unable to overcome the surface tension of the solution. Similarly, the polymer concentration in the solution could either hinder the production of fibers (if too high, due to the high viscosity), or result in the formation of globules of polymer (if too low). Globules of polymer will also form in case the flow rate is too high; conversely, if the flow rate is too low, then this will result into inconsistent deposition of the fibers onto the collector. Furthermore, setup parameters such as the needle diameter and the collector speed exhibit a strong influence on the diameter of the fibers as well as their alignment.<sup>[4,8]</sup>

## 2. Molecularly Imprinted Electrospun Nanofibers: Challenge Accepted

Molecular imprinting is a versatile technology to introduce tailor-made binding sites within a cross-linked polymer matrix. These binding sites exhibit specific size, three-dimensional shape and chemical functionality, allowing them to recognize and rebind the target molecule (“template”) with high affinity and specificity, thus de facto acting in a similar way as antibodies and natural receptors recognize their antigens and ligands, respectively.<sup>[10]</sup> Introduction of the binding site is normally achieved by performing the polymerization process in the presence of the template, using monomers which exhibit adequate complementary functional groups to the target (for either covalent or non-covalent interactions) as well as cross-linkers. Once the polymerization has been performed, the removal of the template is achieved via suitable washing steps,<sup>[11]</sup> or alternatively, depending on the molecularly imprinted polymer (MIP) format, solid-phase synthesis strategies could also be employed where the template is actually immobilized onto a supporting surface (e.g., glass/silicon or iron oxide).<sup>[12]</sup> A schematic of the process is depicted in **Figure 2**.

It is important at this stage to highlight the fact that molecular imprinting technologies indeed do generate a brand new binding site with an otherwise completely random cross-linked

polymeric matrix. Although specific functional monomers are used to facilitate this interaction with the template, the overall affinity is generated thanks to a combination of shape of the target and binding site, physico-chemical interactions as well as environmental factors (such as temperature, pH, ionic strength, etc.).<sup>[11a,b]</sup> Different is the case of ligand-based binding polymers, where well known binding moieties are introduced within a polymer but this latter is not actually prepared in presence of the target molecules, hence the subsequent binding event is solely relying on the interaction between the binder and its target (e.g., biotin-streptavidin), but a specific binding site is not generated. Ion and metal imprinting, for example, sit on the border amongst the two technologies, and there are some controversial opinions as to whether ion imprinting should be considered a true molecular imprinting approach or not, considering it heavily relies on the presence of specific ligands for the interaction with the metal targets.<sup>[11]</sup> For the sake of this progress report, it has been considered a true molecular imprinting technology. Nonetheless, we would like to invite the readers to refer to more comprehensive reviews on the topic.<sup>[11c,d]</sup> In all cases, however, the final product exhibits extremely high stability and robustness even in harsh environmental conditions, highlighting one of the main reasons why MIPs actually represent a suitable cost-effective alternative in comparison to natural and animal-derived reagents

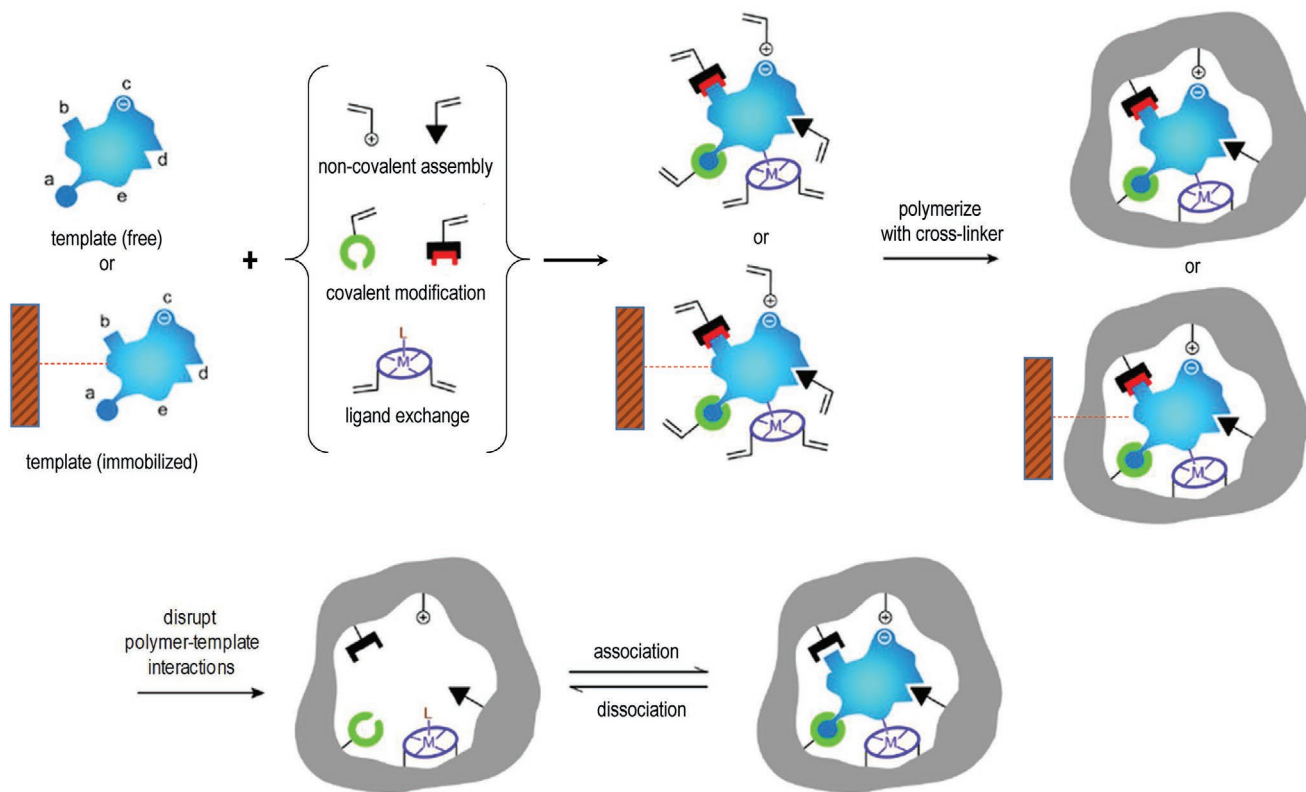


**Figure 2.** Scheme of the molecular imprinting process: the establishment of interactions between the template (free in solution or immobilized on a suitable solid support) and polymerizable groups interacting either covalently, non-covalently, or via co-ordination with a metal center with suitable functional groups or structural elements of the template. Subsequent polymerization in presence of a cross-linker develops a porous insoluble matrix containing the binding sites for the template. At this point, either the template is removed (if free), or alternatively the polymer is separated from the immobilized template in suitable washing/elution conditions. In all cases the target analyte can selectively rebind to the polymer into the sites formed by the template, or “imprints.” Adapted with permission.<sup>[11a]</sup> Copyright 2006, John Wiley & Sons.

(e.g., antibodies).<sup>[13]</sup> Indeed, over the past 50 years MIPs have been reported for a plethora of applications, including solid-phase extraction (SPE) and chromatographic separation,<sup>[14]</sup> recognition of peptides, biomolecules, and even whole cells,<sup>[15]</sup> capturing of hazardous radioactive waste,<sup>[16]</sup> drug delivery,<sup>[17]</sup> and as sensors.<sup>[18]</sup> MIPs produced by conventional bulk polymerization methods, however, historically suffer from low adsorption capacity and slow mass-transfer rates, hence the conjugation of MIP technology with electrospinning to produce micro/nanofibers embedded with inherent specific recognition capacity is certainly extremely attractive, especially for specific separation purposes, sensing applications or even tissue engineering and drug delivery. Nonetheless, the extremely diverse process parameters to adjust for producing MIPs in comparison to the electrospinning technique represent perhaps the major challenge for the conjugation of the two technologies, and over the past few years many approaches and applications have been investigated and reviewed.<sup>[19]</sup> Here we will focus on the pragmatic perspective of the topic, discussing the practical challenges as well as highlighting the most promising research avenues for the conjugation of these two technologies, which are extremely promising for large-scale manufacturing applications and hence certainly deserving of attention.

### 3. How to Prepare MIP Electrospun Nanofibers

The main approaches to produce MIPs via electrospinning can be summarized into the following four main categories: molecular imprinting during the electrospinning process (Figure 3a); development of a MIP layer on the surface of electrospun micro/nanofibers (Figure 3b); solid-phase imprinting approaches (Figure 3c), and dispersion/conjugation of MIP micro- or nanoparticles (MIP NPs) into/onto electrospun micro/nanofibers (Figure 3d). Each of these approaches has its own advantages and disadvantages, mainly deriving from the different processing parameters which characterize the two technologies, and will be discussed more in detail in the following sections.

#### 3.1. Molecular Imprinting during Electrospinning

Intuitively, this approach would represent the most feasible (i.e., dispersing a template within the electrospinning solution and wash the final fiber mat), while in reality it is the most complicated and difficult to achieve, due to the inherent differences between MIP and electrospinning technologies, as previously mentioned. MIPs are by definition cross-linked matrixes, and although there are examples in literature where loose cross-linking or even no cross-linking has been reported, this is not something that is very frequent or easy to perform.<sup>[20]</sup> A cross-linked polymer structure by definition is not soluble, hence it cannot be electrospun. Nonetheless, the production of electrospun poly(ethylene terephthalate) (PET)/polyethylenimine (PEI) nanofibers has been reported by homogeneously dissolving a MIP based on styrene/divinylbenzene imprinted for metal tetraphenylporphyrins before electrospinning.<sup>[21]</sup> It is not perfectly clear, however, the modality which allowed

to introduce the preformed cross-linked imprinted polymer within the electrospun matrixes.

There are, however, some alternatives to the classical cross-linking required by MIPs to perform the electrospinning process in the presence of the template. One of them is to exploit strong interactions amongst the main non-cross-linked polymer chains, as well as interactions between the polymer and the template.<sup>[22]</sup> This would actually guarantee achieving a homogeneous distribution of the binding sites within the fibers. Lack of cross-linking, however, could result in structural alteration of the recognition cavities and, consequently, of the performance of the product.<sup>[22c]</sup> Nonetheless, many successful examples have been reported in the literature, especially when the conjugation amongst these two technologies was first attempted.

MIP nanofibers imprinted for the herbicide 2,4-dichlorophenoxyacetic acid (2,4-D) or the nitroaromatic compound 2,4-dinitrotoluene (DNT) have been successfully prepared by using a mixture of PET as supporting matrix and poly(allylamine) (PAA) as functional macromer.<sup>[22a,23]</sup> The binding site structure integrity in the absence of a cross-linker was stabilized by the strong dipole–dipole interactions between the  $\pi$ -electron systems of the benzene rings and the carbonyl groups in the PET backbone. A similar strategy was also exploited by Kim et al. who relied on the strong interactions between the polymer chains of an aromatic polyimide matrix to covalently imprint estrone for subsequent electrospinning into nanofibers.<sup>[22c]</sup> Non-crosslinked MIP nanofibers produced from polystyrene (PS)<sup>[24]</sup> and poly(ethylene *co*-vinyl alcohol) (EVOH)<sup>[25]</sup> have also been reported.

Yoshikawa et al. successfully prepared electrospun MIP micro- and nanofibrous membranes without cross-linking from carboxylated polysulfone (PSf),<sup>[22b]</sup> polysulfone-aldehyde (PSf-CHO),<sup>[26]</sup> cellulose acetate (CA)<sup>[27]</sup> or chitosan<sup>[28]</sup> for the enantiomeric resolution of *N*- $\alpha$ -benzyloxycarbonyl-glutamic acid and phenylalanine, even using a complex co-axial, two-capillary spinneret which resulted in a core-shell architecture, aimed at localizing the imprinted sites at the surface of the nanofibers.<sup>[28]</sup> However, in all cases the diameter of the fibers obtained was extremely variable, with evident areas of polymer “beading.”

The exploitation of peculiar monomers (e.g., vinyl porphyrins, histidine moieties,  $\beta$ -cyclodextrins, room temperature ionic liquids) and/or polymers (e.g., wool keratose/silk fibroin blends, sericin, chitosan, aramid) with high inherent affinity for certain ions/molecules can be exploited to effectively prepare electrospun MIP nanofibers for these targets, thus overcoming the lack of cross-linking.<sup>[29]</sup> To improve the spinnability, poly(vinyl alcohol) (PVA) can be mixed within the electrospinning solution (e.g., with chitosan or sericin).<sup>[30]</sup> In the case of sol-gel membranes, Nylon 6 was also used for this purpose.<sup>[31]</sup>

Alternatively, cross-linking of the final produced fibers can be carried out post-electrospinning (e.g., via glutaraldehyde or polycondensation), thus achieving not only a stabilization of the recognition cavities, but also an overall increase of mechanical strength of the final fiber mats.<sup>[30–32]</sup> This cross-linking, however, needs to be carefully optimized, since too high levels could actually be counterproductive and result in the formation of brittle fiber mats, too fragile or unsuitable for certain applications where mechanical stress is received from the materials.

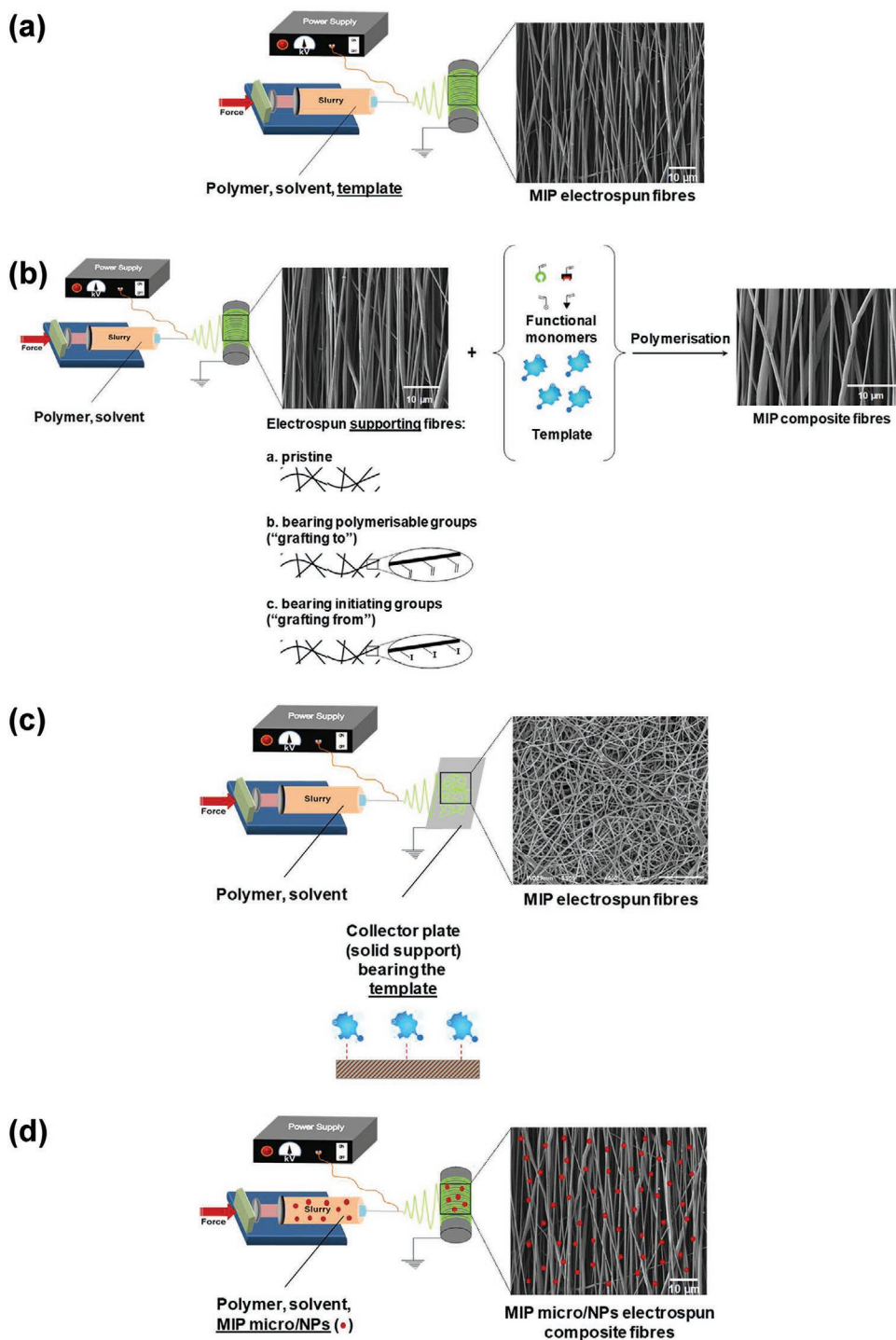


**Figure 3.** Scheme of the four main approaches to produce MIPs via electrospinning: a) molecular imprinting during the electrospinning process (the template is solubilized within the electrospinning solution); b) development of a MIP layer on the surface of electrospun micro/nanofibers which act as a support for the MIP, which is produced either in absence of specific interactions with the support (pristine), or via specific grafting approaches where either polymerizable groups ("grafting to") or initiating moieties ("grafting from") are present on the surface of the supporting electrospun fibers; solid-phase imprinting approaches where the template is immobilized onto the collection medium for the electrospun product and mechanically removed; d) dispersion/conjugation of MIP micro- or nanoparticles (MIP NPs) into/onto electrospun micro/nanofibers. Please note that the micrographs provided are solely for illustration/schematic purposes.

Although cross-linking during the electrospinning process has been attempted, this has actually resulted in reduced binding capacity for the targets.<sup>[32b–d]</sup>

Another alternative to cross-linking could be the collection of the imprinted nanofibers into a non-solvent, such as polyethersulfone (PES) in water.<sup>[33]</sup> Nonetheless, this approach

is far from being risk-free, because it could wholly entrap the template within the precipitated polymer entanglement, thus contaminating the final product or resulting in leaching during the application. For this reason, extremely thorough and lengthy template removal procedures would be required.<sup>[33]</sup>

Similarly, considering the fact that the electrospinning process results in the evaporation of most of the solvent, this could actually promote the precipitation/crystallization of the template during the process (as in the case of theophylline (THO)-imprinted poly(acrylonitrile-co-acrylic acid) (PANCAA)), which in turn could be entrapped within the polymer matrix and also alter the final structure of the imprinted sites or possibly the overall mechanical stability of the final membrane product.<sup>[34]</sup>

Moreover, the need for the exploitation of pre-existing strong interactions between the polymer and the template could actually nullify the scope of the imprinting process altogether, or needlessly overcomplicate it with synthetic modifications of the polymer itself or even the template.<sup>[22c]</sup> Therefore, de facto, this makes the simultaneous molecular imprinting/electrospinning strategy amongst the least popular when attempting to conjugate the two technologies.

### 3.2. MIP Layer Formation onto Electrospun Micro/Nanofibers

Considering the disadvantages highlighted above, an alternative approach for the production of MIP-enabled electrospun fibers is represented by the separate production of a MIP layer onto a preformed electrospun fiber mat. Indeed, when the generation of high-affinity binding sites is hindered by the control of the other parameters of the materials, it is extremely advantageous to separate the imprinting process from the generation of the material itself (e.g., membrane, particle, or sensor) characterized by a precise morphology.<sup>[35]</sup> Three possibilities could be exploited to achieve this: a simple preparation of a MIP layer onto the electrospun support, without the presence of specific chemical interactions, or alternatively a chemical grafting, either “to” or “from” an electrospun support.<sup>[36]</sup>

Zhai et al.<sup>[37]</sup> exploited the first possibility to produce electrospun nanofibers of CA/multi-walled carbon nanotubes (MWCNTs)/polyvinylpyrrolidone (PVP) (CA/MWCNTs/PVP) which were then decorated with an electropolymerized polypyrrole layer imprinted for the template, ascorbic acid (AA). Similarly, Wu et al. exploited a PES electrospun nanofiber mat as supporting material to produce a polydopamine bilirubin-imprinted MIP layer via the spontaneous polymerization of dopamine in weak alkaline conditions.<sup>[38]</sup>

However, a drawback of this extremely simple procedure is represented by the potential low physico-chemical robustness and potential susceptibility of the recognition layer to degradation, particularly if intended for long-term applications.

From this point of view, the “grafting” approaches guarantee the establishment of an actual chemical bond between the electrospun layer and the MIP. In particular, the grafting “to” approach involves the reaction between the end-functional groups of the imprinted polymer chains growing in solution and suitable functional groups immobilized on the support (usually vinyl ones). Unfortunately, this method usually does not allow depositing a sufficient amount of polymer onto the

surface of the support. Moreover, at the same time, uncontrolled bulk polymerization might take place in solution.<sup>[39]</sup>

The grafting “from” technique, instead, requires that the polymerization process starts from the support using an initiator moiety immobilized on its surface. This usually results in layers characterized by higher amounts of grafted imprinted polymer chains, and in turn higher binding capacity.<sup>[40]</sup> Although both approaches have been exploited and demonstrated for the formation of MIP membranes as well as core-shell micro/nanoparticle architectures;<sup>[35,39–40]</sup> unfortunately, no reports are available in the case of electrospun fiber mats. This could be due to the challenges of achieving post-electrospinning chemical modifications of the materials. Indeed, in the case of a grafting “to” approach it could be extremely difficult to control the polymerization process to form the imprinted polymer without affecting the porosity of the fiber mat. However, in the case of the grafting “from” approach, there would be a much higher control of the polymerization process, which should result in a higher performance of the final composite material. Also in this case, however, there might be issues arising from the occlusion of the membrane pores or fusion of the adjacent fibers, which might hinder the subsequent application as well as the template removal steps, hence careful optimization of the grafting conditions should be performed. Nonetheless, it would be certainly interesting to investigate this approach, also considering that it would be extremely innovative in the case of MIP electrospun composites.

### 3.3. Solid-Phase Imprinting Strategies

To negate the heterogeneous affinity distribution of MIPs (due to the translational and rotational motion of soluble templates during polymerization) as well as to the difficulty of access of binding sites when exploiting a bulk polymerization approach,<sup>[41]</sup> a recent trend for MIPs production exploits the covalent immobilization of the template on a suitable support. This expands the range of solvents that can be used in molecular imprinting (which might be particularly advantageous for electrospinning) and suppresses also template–template interactions. Most importantly, however, immobilized templates are less motile, they can be oriented and the polymerization happens at the interface with the template support, thus increasing the binding sites accessibility during the application as well as for template removal.<sup>[12a–c,42]</sup>

When solid-phase imprinting is used, the solid support bearing the template can be either retained or sacrificed. In this latter case, the imprinting process is defined as “hierarchical imprinting.”

An extremely interesting application of hierarchical imprinting conjugated to electrospinning was reported by Zhu et al. for protein separation.<sup>[43]</sup> Indeed, the authors have cleverly used an electrospun PVP/silica mat bearing the target protein [bovine serum albumin (BSA) or bovine hemoglobin (bHb)], as sacrificial template to generate polyacrylamide-based MIP membranes with enhanced porosity and extremely high accessibility to the binding sites. Since the electrospun membranes exhibit a high-specific surface area, conversely the diameter of the “tubular cavities” produced after removal of the solid phase can be easily controlled. Indeed, the authors tailored the

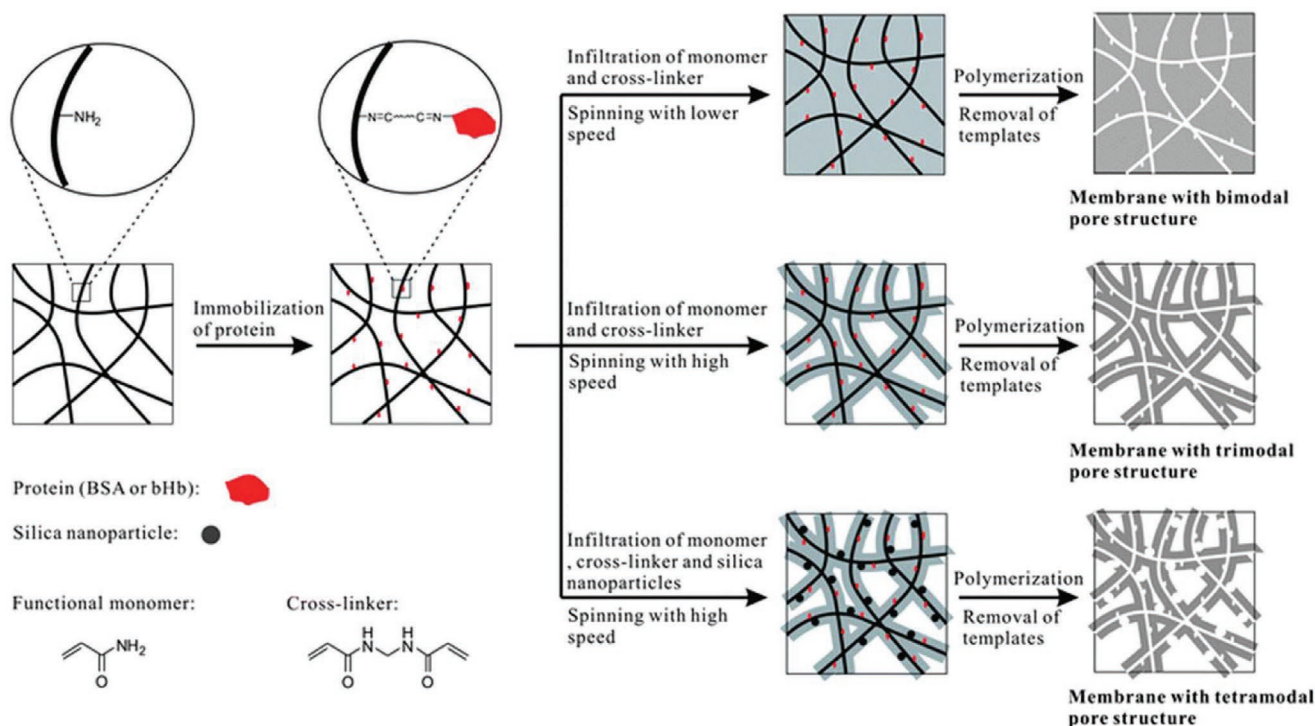


**Figure 4.** Schematic illustration of the preparation of surface molecularly imprinted affinity membranes with bi-, tri-, and tetramodal pore structures. Adapted with permission.<sup>[43]</sup> Copyright 2013, Royal Society of Chemistry.

production of imprinted fibrous membranes with bi-, tri- or tetramodal pore structures by adjusting the composition of the polymerization mixture (e.g., with or without the addition of silica nanoparticles) as well as the spin-coating parameters used to introduce the polymerization mixture within the electrospun fiber mat (Figure 4).

However, despite the discussed advantages, the hierarchical imprinting approach does not provide benefits from an economical and synthetic point of view when compared with a normal imprinting procedure with a free template in solution. The template molecules are still discarded at the end of the MIP synthesis, together with the solid support, which might require harsh treatments for its dissolution (e.g., concentrated hydrofluoric acid).

A more sustainable approach is represented by the usage of a recyclable solid-phase, as reported by Criscenti et al., who fabricated a soft-molecular imprinted electrospun bioactive scaffold (SMIES) using poly(lactic-co-glycolic acid) (PLGA) imprinted with physiological proteins and growth factors.<sup>[44]</sup> More in detail, the authors first produced a mold in polydimethylsiloxane (PDMS) via soft lithography, which was subsequently functionalized with amino groups and conjugated to the protein templates previously activated via 1-ethyl-3-(3-dimethylaminopropyl)carbodiimide and *N*-hydroxysuccinimide.<sup>[45]</sup> This mold was then exploited as a solid phase onto which the electrospun imprinted PLGA mat was deposited (Figure 5).

This recent approach seems quite promising to easily conjugate molecular imprinting and electrospinning, because it allows to easily remove the templates and also to potentially reuse the solid phase (although this has not been assessed by the authors of the study). Advantageously, the process parameters

for imprinting and electrospinning are kept separate, but also in this case no cross-linking was performed, even though it could be implemented post-electrospinning. The usage of the soft lithography allows to introduce a further level of control within the system, which is extremely important for the development of specific micro/nanoarchitectures.<sup>[46]</sup> It would be interesting, however, to actually assess the possibility of using simpler solid phases (e.g., plain glass) for basic large-scale MIP electrospinning applications (such as separation/purification).

### 3.4. Dispersion/Conjugation of MIP Microparticles or MIP NPs into/onto Electrospun Micro/Nanofibers

This approach is perhaps the most investigated to introduce recognition properties based on molecular imprinting within electrospun fiber mats. Indeed, it is extremely easy to perform, separating the process parameters for the two technologies and thus being easily tailorable to achieve the desired final architecture coupled to an efficient recognition performance.

Briefly, two simple steps can be identified: the first one is the production of MIP microparticles or MIP NPs, which are subsequently conjugated with electrospun fiber mats either by immobilization onto their surface or, more frequently, by embedding within their structure thanks to the previous dispersion into the electrospinning solution.

One of the first examples of this approach was reported by Chronakis et al. in 2006, who encapsulated MIP NPs produced via precipitation polymerization and imprinted for THO or 17 $\beta$ -estradiol (ES) within PET nanofibers, up to 70% in weight and without evident NPs loss from the fibers. Indeed, MIP NPs

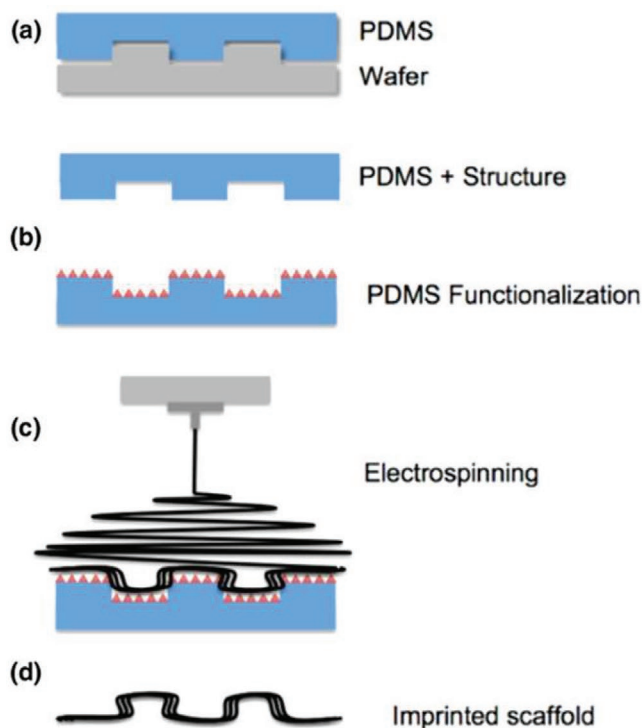


**Figure 5.** Schematic illustration of the SMIES fabrication process: a) soft lithography process for the fabrication of PDMS molds; b) functionalization of PDMS molds with the template molecules; c) electrospinning of the polymer solution on top of the functionalized PDMS molds; d) removal of the electrospun scaffolds from the molds to obtain the imprinted scaffolds. Reproduced with permission.<sup>[44]</sup> Copyright 2018, IOP Publishing.

could be visually identified within the fiber structures via scanning electron microscopy.<sup>[47]</sup>

From this moment onward, many more groups have employed this strategy to conjugate the two technologies, imprinting a variety of compounds and using different polymer matrixes (including PS, polyacrylonitrile and even biodegradable PVA and PCL).<sup>[48]</sup>

Although MIP microparticles can also be embedded within electrospun nanofibers, this is normally more difficult to achieve due to their comparably large size, and frequently results in challenging aggregation and uneven distribution phenomena within the electrospun matrix, although these appear to be also dependent on the concentration of microspheres used for the electrospinning process.<sup>[48a,49]</sup> In this case, perhaps it would be better to prepare electrospun mats with larger fiber diameters, also ensuring the suspension stability of the microparticles in the electrospinning slurry.<sup>[50]</sup>

Normally, MIP micro or NPs produced via specific “bottom-up” tailored polymerization processes (i.e., starting from the monomers) are used for their integration within the electrospun materials, such as precipitation polymerization or emulsion and mini-emulsion polymerization.<sup>[48a,e,h,k,50–51]</sup> Indeed, these strategies are quite established, providing narrow particle-size distributions with final products characterized by reproducible performance.<sup>[49]</sup> Nonetheless, also “top-down” approaches (where microparticles derive from the grinding and sieving of

bulk imprinted polymers) were used, although the classical drawbacks that burden bulk MIPs in this case are simply transferred to the final electrospun composite products with almost no room for performance improvement.<sup>[48j,52]</sup> A silver lining might be represented by resorting to surface-immobilization strategies of the MIP particles onto the electrospun fiber mats, instead of incorporating them within the fibers. This should improve the binding sites accessibility and overall increase the performance of the material in comparison to the bulk MIP counterpart. Nonetheless, in the absence of excellent-performing bulk MIPs to begin with, the recognition characteristics of the composite electrospun membranes cannot be dramatically improved, even though the global applicability of the system can profit from improved flexibility.<sup>[48i]</sup>

On the other hand, when the starting MIP microparticles or MIP NPs are produced with a bottom-up strategy as the ones described above, the overall recognition performance of the electrospun composite is generally excellent.<sup>[48k]</sup>

Nonetheless, “all that glitters is not gold,” and also this approach requires careful optimization of the synthetic and production parameters to avoid drawbacks. First, it is important to adequately balance the dispersion of the MIP particles within the electrospinning solution to achieve homogeneous distribution within the fibers. Second, it is critical to avoid a complete coverage and occlusion of the binding sites, but simultaneously ensuring that the MIP particles are adequately supported within the electrospun matrix to avoid losses during the usage.<sup>[47]</sup> A similar effect has to be considered for the overall recognition performance, taking into account that the non-imprinted polymer support could actually contribute to non-specific recognition interactions with the target molecules during the applications.<sup>[47]</sup> Moreover, a modification of the physico-chemical as well as recognition properties of the MIP particles could take place due to their incorporation (in terms of swelling, size, affinity, and porosity).<sup>[48e]</sup>

Nevertheless, the advantages of this MIP microparticles/NPs encapsulation/immobilization approach with electrospun fibers seem to largely outweigh the drawbacks. In addition to the benefits in terms of flexibility and ease, the possibility of dramatically altering the solvent compatibility of MIPs by dispersing the particles in an outer matrix with suitable properties (e.g., hydrophobic MIP NPs dispersed in a hydrophilic matrix for applications in water)<sup>[48f]</sup> or the possibility of combining different recognition capabilities by simultaneously encapsulating particles imprinted for different or incompatible templates within the same matrix are certainly extremely attractive advantages.<sup>[48g]</sup>

## 4. Applications of Molecularly Imprinted Electrospun Polymers

### 4.1. Enhanced Chemical Purification and Preconcentration

#### 4.1.1. Pesticides/Herbicides, Food/Environmental Contaminants, Drugs, Proteins

One of the first examples of molecularly imprinted polymers prepared by electrospinning for chemical purification

applications has been reported by Chronakis et al. in 2006,<sup>[22a]</sup> who prepared MIP electrospun nanofibers imprinted for the herbicide 2,4-D. Although used mainly as a model compound, this first example paves the way for the development of MIP electrospun nanofibers for separation and purification purposes, especially for industrial filtration. Indeed, the presence of selective molecular recognition sites into the fiber mats could provide highly efficient compound separation involving only a simple filtration step. For instance, the centrifugation step commonly used to separate sequestering particles from solution can be omitted.<sup>[19d]</sup>

Herbicide detection and preconcentration is undoubtedly an important area in agriculture, food and water analysis. Ruggieri et al.<sup>[24]</sup> reported the production of PS-based MIP electrospun nanofibers for the pesticide atrazine as template, comparing their performance in the presence of six other pesticides and two commercial adsorbents. The results showed that the commercial phases exhibited a higher affinity for the pesticides at low concentration (although relatively poor selectivity), while the MIP nanofibers were more efficient at high concentrations. Even though commercial phases could be better suited for preconcentration applications, large-scale pesticide purification from wastewater would certainly benefit from this type of MIP electrospun sorbents.

A clever approach for environmental purification and removal of organophosphorous pesticides has been reported by Zhang et al. in 2014.<sup>[48e]</sup> The authors prepared polyacrylonitrile nanofibers with encapsulated MIP NPs imprinted for *p*-nitrophenol, the hydrolysis product of the pesticide paraoxon. The hypothesis behind this work was to directly sequester the environmental pollutant target, while at the same time shifting the hydrolysis reaction equilibrium of paraoxon toward the formation of the products. MIP NPs on their own exhibited a remarkable increase in the hydrolysis rate; however, some of the imprinting effect was lost after incorporation within the electrospun nanofibers, highlighting that this approach, although quite elegant, still requires some optimization.

The nitrocompound DNT is an important chemical intermediate, widely used in organic synthesis. However, DNT is acutely toxic and potentially carcinogenic, hence its trace detection is extremely important for environmental monitoring. Xue et al. developed PET DNT-MIP electrospun nanofibers using PAA as a functional macromer.<sup>[23]</sup> Their results show specific adsorption of DNT, also when in presence of structural analogues such as nitrobenzene, benzoic acid or dinitrobenzoic acid. Moreover, the nanofibers exhibited remarkable stability and reusability (almost no loss of performance after 8 recycles). It would have been useful, however, to assess the performance of the imprinted products on real samples, to verify the recognition capacity within a complex water matrix.

For analytical purposes, drug analysis and preconcentration also are quite attractive applications for MIP electrospun nanofibers. Chronakis et al. encapsulated MIP NPs imprinted for THO or ES within the fibers.<sup>[47]</sup> The rebinding levels of MIP composites were two- to threefold higher than non-imprinted materials, but the solvent dependency of the binding was difficult to predict, highlighting the need for careful optimization to prepare a final purification product which would consistently perform at high-scale.

A successful application in the drug analysis area was reported for the preconcentration of samples of the drug propranolol via a modified SPE process,<sup>[19a]</sup> where MIP NPs-embedded fiber mats were employed instead of the classical packing materials.<sup>[48a]</sup> MIP composite nanofibers were able to bind up to sixfold more target compound than the non-imprinted ones, proportionally to the mass of encapsulated MIP NPs. Most importantly, they exhibited a promising degree of enantioselectivity, which is extremely difficult to achieve even when imprinting enantiomerically pure templates.<sup>[22b]</sup> Furthermore, they could be reused for consistent selective preconcentration of spiked tap water samples for more than 10 times, allowing to detect the analyte (otherwise undetectable by HPLC-MS/MS analysis). Given that nanofiber membranes can be easily integrated into small filter units, these affinity materials are expected to find broader applications for pre-treatment of more complex samples (e.g., to analyze drug metabolites in biological fluids and for safety control of food products).

To maximize the analytical output, Moein et al. integrated their composite MIP electrospun membrane for the sweetener acesulfame on-line with the HPLC system, thus achieving automatic and standardized preconcentration before the analysis of the samples (up to 50 consecutive cycles without loss of enrichment capability).<sup>[31]</sup> Although various parameters have to be optimized to achieve the best preconcentration performance, a final enrichment of 85–96% was achieved (of analyte in the processed injected sample in comparison to its initial concentration) with an imprinting factor (IF) of 4.25. Moreover, up to fourfold higher selectivity for acesulfame was reported in comparison to other sweeteners.

Detection of trace amounts of bisphenol A (BPA) is extremely important for food and water safety, and has been thoroughly investigated through various techniques, including MIP electrospun nanofibers.<sup>[29b,33,48f]</sup> Wu et al. have actually raised the bar for the challenge and reported a MIP electrospun nanofiber system simultaneously imprinted for BPA and tebuconazole (TBZ, a fungicide with potential reproductive toxicity and carcinogenicity) for SPE and detection in food samples.<sup>[48g]</sup> The authors exploited the contemporary encapsulation of MIP NPs imprinted singularly for each template into the electrospun PVA nanofibers. This type of system exhibited a higher binding capacity and selectivity in comparison to the nanofibers encapsulated with MIP NPs simultaneously imprinted for both templates, although its performance was lower than the single imprinted fibers when tested against each separate target. Nevertheless, the recovery performance was comparable to bulk MIP SPE, and superior to commercial C<sub>18</sub> resins. Nonetheless, further optimization of the synthesis and of the SPE protocol could perhaps improve the performance even further.

An extremely clever approach aimed at bioremediation of BPA-contaminated wastewater has been adopted by Liu et al., who prepared MIP electrospun nanofiber membranes by encapsulating BPA-imprinted MIP NPs into electrospun PVA nanofibers (**Figure 6**).<sup>[48f]</sup>

Placed into water containing BPA and BPA-degrading bacteria, the obtained composites could immobilize BPA-degrading bacteria (*Pseudomonas aeruginosa*) and enrich BPA simultaneously, thus achieving almost complete trace BPA removal over 10 days. Moreover, the recycle of adsorption-degradation could

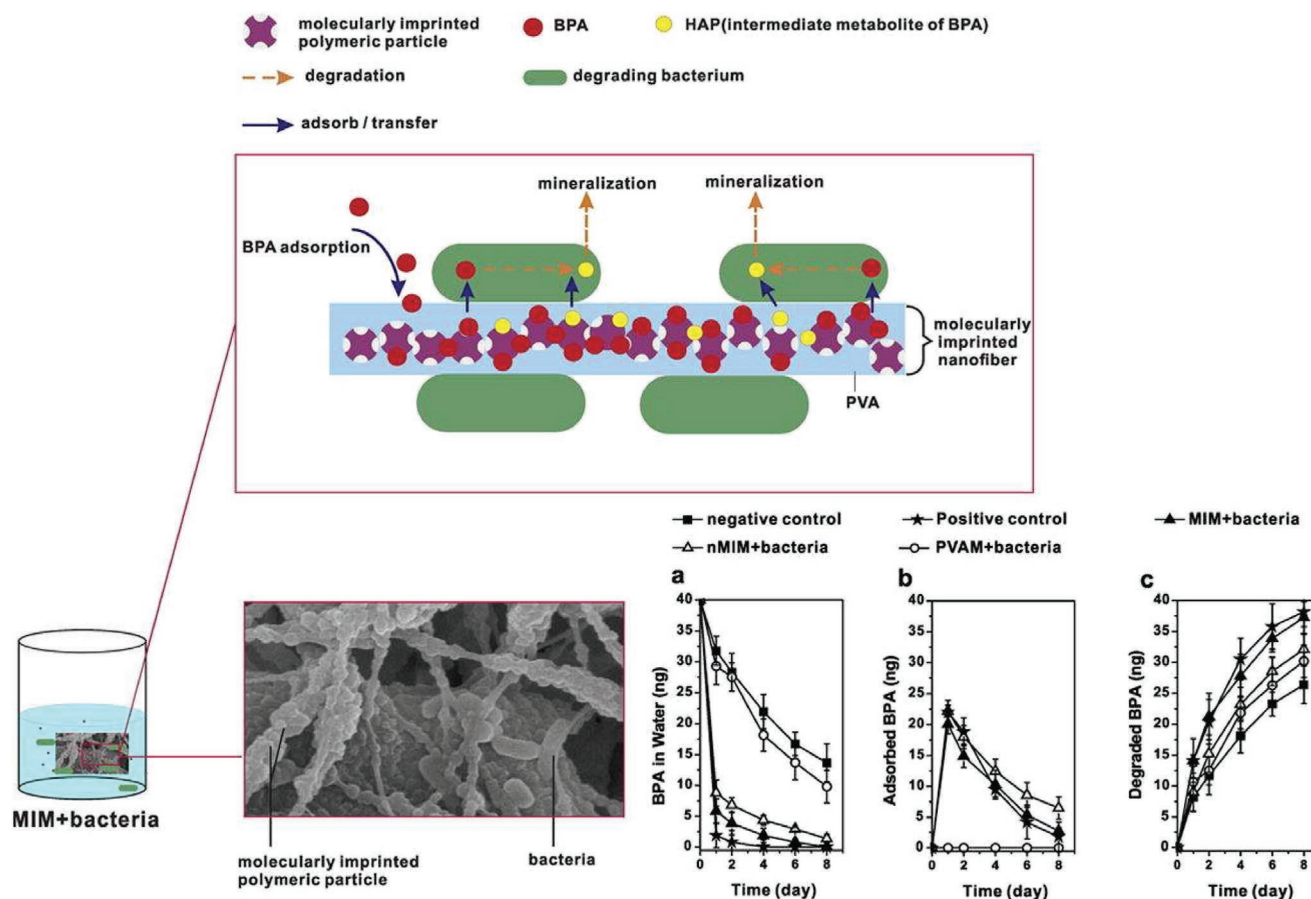


**Figure 6.** Molecularly imprinted nanofiber membranes (MIMs) were used to enhance the degradation of trace BPA by *Pseudomonas aeruginosa* bacteria. MIMs were prepared by encapsulating BPA-imprinted MIP NPs into PVA nanofibers using electrospinning. MIMs could enrich BPA and its intermediate metabolites 4-hydroxyacetophenone (HAP) selectively. FESEM image shows the BPA degrading-bacteria *P. aeruginosa* attached and immobilized on the biocompatible MIMs after 3 h incubation. The graphs depict degradation of BPA in different treated groups: a) BPA levels in water phase; b) adsorbed BPA levels; c) degraded BPA levels. The initial BPA level was  $50 \mu\text{g L}^{-1}$ . The MIMs pre-immobilized with  $4 \times 10^8$  bacteria were used as a positive control, and a membrane-free bacteria suspension ( $\approx 4 \times 10^8$  bacteria) was used as a negative control. nMIM, non-imprinted nanofiber membrane; PVAM, PVA nanofibrous membrane. Reproduced with permission.<sup>[48f]</sup> Copyright 2015, Elsevier.

actually regenerate the sorbents in the MIP membranes, thus retaining their high adsorption capability. The membrane performance, however, was negatively influenced by the presence of heavy metals or other toxic contaminants in the wastewater, even though this was mainly due to the toxic effect on the bacteria themselves rather than on the adsorption capacity of the imprinted material.

An enhanced performance for water purification applications has been reported by Wei et al.<sup>[29b]</sup> These authors have assessed the possibility of using MIP aramid nanofibers imprinted for BPA. Although the selectivity for smaller structural analogues was poor, an imprinting factor of 3.6 was achieved for the target, highlighting the promising possibility of optimizing these types of imprinted electrospun nanomaterials for purification and/or detection applications.

Instead of sugars, Zhao et al. exploited protein fibers, specifically sericin/PVA electrospun fibers imprinted for methylene blue.<sup>[30a]</sup> In a comparison study with control nanofibers, MIPs showed an enhanced and selective adsorption capacity (imprinting factor of 2.1, with selectivity for competing dyes

above 1.8 and up to 4.4) toward methylene blue with a good regeneration and recycling ability (94% retention after 5 cycles). This sustainable system is extremely promising for the large-scale selective purification of dyes from wastewater.

Separation applications have been pursued also with electrospun fibers embedded with MIP microparticles, for the purification/preconcentration of rhodamine B,<sup>[48d]</sup> propranolol<sup>[50]</sup> or (–)-cinchonidine.<sup>[49]</sup> In this latter case, although the accessibility for the template was maintained, the difference in rebinding between MIP and control membranes was not massive. Moreover, no selectivity rebinding studies were performed. Interestingly, the location of the binding of the template within the composite membrane could be visualized via Raman microscopy, which could be of significant importance for sensing/imaging applications. Although a promising example, further experiments need to be performed to ensure the reliability of the approach.

The same type of architecture was recently exploited by Demirkurt et al. for the selective preconcentration of parabens from water samples.<sup>[48k]</sup> The MIP composite products exhibited

attractive imprinting behavior, with 250 mg g<sup>-1</sup> binding capacity for the targets, and limits of detection (LODs) obtained in the range 0.26–0.29 ng mL<sup>-1</sup>. However, the recycling potential was poor in comparison to commercial SPE silica microfibers, and although the MIP products developed by the authors were up to threefold more selective when tested in the presence of interfering substances, for analytical intensive applications such poor reusability could represent an obstacle in terms of time-efficiency as well as from a financial perspective.

An extremely interesting application of electrospinning applied to MIP technology was reported by Zhu et al. for protein separation.<sup>[43]</sup> The purification performance of the final membranes for the targets (BSA or bHb) was remarkable during dynamic adsorption cycles, with a reduction of 50% of the protein concentration after eight cycles. Moreover, the materials could be recycled without dramatically losing adsorption capacity when used in batch mode (≈10% after six cycles). Nonetheless, the production method (see Section 3.3) would most likely be inefficient from an economical perspective to translate this technology for large-scale protein separation applications, thus confining this approach purely to an academic exercise.

#### 4.1.2. Enantioseparation

Optical resolution is extremely difficult to achieve, especially in the case of a solution filtering through a membrane.<sup>[53]</sup> Nonetheless, a first preliminary approach toward this application was reported by Yoshikawa et al., who prepared PSf and PSf-CHO electrospun MIP microfiber membranes imprinted for *N*- $\alpha$ -benzyloxycarbonyl-L-glutamic acid or its d-isomer.<sup>[22b]</sup> MIP electrospun membranes selectively recognized each enantiomer in presence of the corresponding isomer to a certain extent (enantioselectivity up to 1.4), but most importantly, the imprinted amino acid was selectively transported through the membrane according to its concentration gradient, although the permselectivity (i.e., the preferential permeation of a certain species through a membrane) was not too high (1.15–1.20). Curiously, the mobility was “inverted” in the case of PSf-CHO membranes, that is, the imprinted enantiomer was retained during transport, while the other isomer would cross the membrane more rapidly.<sup>[26]</sup> Perhaps the aldehyde group would alter the type of retention during the binding event. In a subsequent study, the same authors modified the approach by adopting CA instead of PSf.<sup>[27]</sup> The produced membranes successfully and selectively separated the two enantiomers to a certain extent (selectivity values during permeation were ≈1.45 for both enantiomers), with a flux value (molar mobility, *u*) which was one to two orders of magnitude higher than the previous results but without a dramatic reduction of permselectivity. It is likely that the overall performance of these membranes could be improved with careful optimization of preparation conditions and experimental parameters (e.g., by reducing the fiber diameter, thus increasing the surface area and number of recognition sites).

The same group investigated the possibility of modifying the architecture of the membranes to enhance the enantioselectivity. Chitosan-based MIP electrospun nanofibers were prepared for L- or D-phenylalanine, either with the classical approach and also with a more complex core-shell architecture, aimed at

localizing the imprinted sites at the surface of the nanofibers.<sup>[28]</sup> However, against the authors hypothesis, the core-shell MIP nanofibers did not exhibit enhanced enantioselectivity (neither during static adsorption nor in flux). Perhaps more optimization studies are required to obtain the best performing architecture. In addition, it might be interesting to actually attempt the core-shell permeation with the same previous templates and polymer composition, thus obtaining a more systematic comparison with previous data.

Alternatively, MIP electrospun fibers could be exploited to achieve purification via selective crystallization. Che et al. in 2006<sup>[34]</sup> pursued this application by preparing MIP nanofibers imprinted for THO, and subsequently using them to guide the selective recrystallization of the template from supersaturated solutions. Although this type of application could be potentially ground-breaking in the selective crystallization of difficult to obtain or, even more audaciously, of enantiomerically pure compounds from racemic solutions, it was never investigated further.

#### 4.1.3. Fuel Desulfurization

Oxidized sulfur-containing compounds were also imprinted on chitosan MIP electrospun nanofibers for the desulfurization of fuels.<sup>[29c]</sup> Although the MIP nanofibers were applied to oxidized hydro-treated fuel under continuous flow (1 mL h<sup>-1</sup>), adsorbing 84% of sulfur (adsorption capacity of 2.2 ± 0.2 mg g<sup>-1</sup>), in reality the non-imprinted materials exhibited a higher capacity for sulfur compounds during a first usage. These latter, however, could not be recycled, while the MIP nanofibers maintained their adsorption capacity almost the same even after recycling. In this case, perhaps, a better optimization of the imprinting process would improve the adsorption capacity of the MIP matrixes, or alternatively the usage of disposable non-imprinted adsorbents in batch-mode rather than continuous flow might result in a better final performance. The selectivity factors, however, were quite satisfactory, up to 4.9 for the smallest imprinted sulfone templates.

## 4.2. Heavy Metal Purification

The exploitation of peculiar monomers with high affinity for certain ions (e.g., Zn<sup>+2</sup>, Cu<sup>+2</sup>, Pb<sup>+2</sup>, Ni<sup>+2</sup>, Vn<sup>+2</sup>, Cd<sup>+2</sup>, Th<sup>+4</sup>, or Cr<sup>+6</sup>) can be exploited to prepare MIP fibers suitable for heavy metal purification/preconcentration, catalysis, and light/energy conversion applications.<sup>[29a]</sup>

Ki et al. exploited the amino acidic variability of wool keratose/silk fibroin blends to generate electrospun membranes for Cu<sup>+2</sup> purification from water.<sup>[32a]</sup> The authors confirmed the high capacity of the newly produced membranes in comparison to standard filtration materials, but most importantly the excellent possibility of regeneration of the membrane (tested up to six times with more than 90% recycling efficiency). It would have been interesting to directly compare the membrane performance to existing commercial ion adsorbents, to potentially estimate if a similar approach would be cost-effective for large-scale applications.

Using a more targeted selection for the binding moiety, Liu et al.<sup>[30b]</sup> prepared Cu<sup>+2</sup> imprinted PVA electrospun nanofibers bearing histidine moieties. Although a high binding capacity for Cu<sup>+2</sup> was achieved, this was quite dependent on the pH and the ionization status of the histidine imidazole ring, as well as the temperature. Nevertheless, high selectivity values were achieved when in presence of competing ionic species (selectivity factors of 51.6, 54.4, and 66.3 for Pb<sup>+2</sup>, Ni<sup>+2</sup> and Zn<sup>+2</sup>, respectively), and satisfactory regeneration properties (tested up to five times with 88% recycling efficiency).

Rammika et al.<sup>[52]</sup> similarly exploited dimethylglyoxime-bearing Ni<sup>+2</sup>-imprinted particles dispersed within polysulfone electrospun nanofiber mats for SPE and purification from water, achieving recovery rates above 90% even in the presence of interfering ions. However, the imprinting effect and the selectivity were not impressive (MIP membranes bound 1.4-fold more ions than control ones, and highest selectivity factor was 2.1). Perhaps a different formulation of the particles (e.g., via a “bottom-up” synthetic approach) or the usage of a different polymer backbone for the fibers could improve this performance.

Li et al. focused their attention on Pb<sup>+2</sup> and Cd<sup>+2</sup> removal from wastewater by revisiting chitosan as adsorbent.<sup>[32b-d]</sup> The final mats were applied for the adsorption of Pb<sup>+2</sup> ions in solution, achieving the highest reported adsorption capacity of 570 mg g<sup>-1</sup> (364.3 mg g<sup>-1</sup> for Cd<sup>+2</sup>), although this value could not stand multiple regeneration cycles and dropped by ≈80% at the third recycle. Furthermore, a certain degree of cross-reactivity with other bivalent ions was observed, and partial degradation was observed depending on the pH and the cross-linking degree. Further optimization of the production/separation parameters is undoubtedly required to ensure the product can consistently perform for large-scale purification applications.

Rather than water, Awokoya et al. applied electrospun PET/PEI MIP nanofibers to the removal of nickel-5,10,15,20-tetra-phenylporphine (NTPP)<sup>[21a]</sup> or the simultaneous removal of NTPP and vanadyl tetraphenylporphyrin (VTPP)<sup>[21b]</sup> from oil. Indeed, trace metals such as nickel and vanadium can have significant and detrimental effects on the refining process of oil and can cause environmental pollution. The authors found that the NTPP adsorption capacity increased proportionally to the molar ratio of NTPP to styrene, with an optimal ratio of template to functional monomer [which yielded the best specific affinity and the highest recovery (>99%)] of 3:1. However, it is not perfectly detailed at which stage the imprinted polymer is introduced/produced within the electrospun matrixes. Moreover, a certain dependence from the polarity of the extraction solvent has been observed. Nonetheless, the authors report imprinting factors of up to 5.6, with almost complete recovery and recyclability up to nine consecutive cycles. Further investigations, however, should be performed to validate the approach and better explain the production and recognition mechanism.

Gore et al.<sup>[30c]</sup> have recently explored the possibility of using chitosan/PVA MIP electrospun nanofibers (with embedded 1-butyl-3-methylimidazolium tetrafluoroborate) for the purification of radioactive waste in the form of Th<sup>+4</sup> ions. The maximum adsorption efficiency exhibited by the MIP nanofibers was 90% (at pH = 7 and 25 °C) within 2 h. Despite thorough modelling and thermodynamic characterization was attained,

the study presents some applicability limitations. Indeed, no real samples purification was attempted nor selectivity measurements or competition with other ionic species. Further experimentations should be performed to assess in depth the performance of the presented materials, especially for large-scale purification of radioactive waste.

Industrial processes such as plating, tanning, paint production, pigment production and metallurgy involve the use of Cr<sup>+6</sup> compounds, which is non-biodegradable and highly toxic and may be involved in the pathogenesis of liver, kidney, lung, and gastrointestinal cancers. With the aim of removing Cr<sup>+6</sup> from wastewater, Cr<sup>+6</sup> MIP particles were grafted on the surface of electrospun polyacrylonitrile and tested.<sup>[48j]</sup> The maximum adsorption capacity of the composite MIP electrospun nanofibers was 398 mg g<sup>-1</sup> (the highest reported in literature), achieved within 12 min, with an impressive IF of 5.7 and the products were extremely selective against interfering species such as Cr<sup>+3</sup>, Cd<sup>+2</sup>, and Cu<sup>+2</sup> (up to 12-fold more selective). Moreover, the produced MIPs were reused up to three consecutive cycles without loss in performance. The performance of this system was astonishing, but it could have benefitted also in this case by the assessment on real samples to verify its performance in the presence of a complex matrix.

### 4.3. Sensing and Signal Transduction

One of the first examples of electrospun-MIPs sensor technology has been reported by Yoshimatsu et al. in 2008,<sup>[48b]</sup> where they developed a proximity scintillation assay by incorporating propranolol-imprinted MIP NPs into electrospun PS nanofibers doped with an organic scintillator (9,10-diphenylanthracene). Although this has been one of the first examples of assays developed using electrospun MIP fibers, its reliability on radioactive tracers makes it poorly applicable nowadays. Nonetheless, it is worth mentioning due to its elegance and interesting performance [IC<sub>50</sub> value for (*S*)-propranolol hydrochloride in human urine spiked samples was 15.5 ± 2.0 μM, with a 9% cross-reactivity with the (*R*)-enantiomer].

An interesting report has been produced by Piperno et al., who optimized a fluorescence assay for the amino acid dansyl-*L*-phenylalanine based on MIP NPs embedded into hydrophilic PVA electrospun nanofibers.<sup>[48c]</sup> The authors measured a dissociation constant (*K*<sub>D</sub>) of 21 ± 5 μM, with a limited degree of enantioselectivity for the target. However, the most important limitation of this study, in our opinion, is represented by the fact that the fluorescence assay is solely relying on the availability of a fluorescent target (and its structural similarity with the parental amino acid *L*-phenylalanine). A radically different strategy would need to be implemented to widen the scope of this fluorescent assay to other molecular targets.

The first integration of a MIP electrospun product with an electrode for diagnostic sensing applications has been investigated by Betatache et al.,<sup>[25]</sup> who elaborated a biomimetic imprinted sensor for impedimetric detection of creatinine by directly electrospinning EVOH onto gold electrodes. The sensor exhibited a linear response toward creatinine in the concentration range from 1 fg L<sup>-1</sup> to 1 μg L<sup>-1</sup>. Some further experiments, however, should be performed to assess the selectivity

in the presence of interfering compounds and the response for structural analogues. Nonetheless, it was possible to reuse the sensor up to three times without loss of performance.

A more recent development entailed the production of an impedimetric sensor based on carbon nanotubes for the gas formaldehyde.<sup>[54]</sup> Formaldehyde is found in many consumer products and greatly affects human health due to its carcinogenic and mutagenic properties.<sup>[55]</sup> The performance of the sensor was remarkable, with a limit of detection of  $0.8 \mu\text{mol L}^{-1}$  and a linear response in the formaldehyde concentration range from  $1 \mu\text{mol L}^{-1}$  to  $10 \text{mmol L}^{-1}$ . Moreover, the sensor exhibited 50 to 100-fold higher selectivity for the target in comparison to interfering compounds (e.g., ions, alcohols or small aldehydes). Careful optimization of the content of carbon nanotubes, however, has to be taken into account to avoid a loss of selectivity.

A similar approach has been exploited by Zhai et al.<sup>[37]</sup> to produce a sensor for AA. Accurate detection of AA is considerably significant for human health and food quality. The performance of the electrochemical sensor was extremely satisfactory in terms of selectivity (up to threefold in comparison to structural analogues) and imprinting effect (3.2). The MIP composite sensors exhibited a linear range of detection for AA between 10.0 and  $1000 \mu\text{M}$ , with an LOD of  $3 \mu\text{M}$  and an almost complete recovery rate from testing on commercial vitamin C tablets. Moreover, up to ten consecutive measurements could be performed without loss of signal performance, as well as storage times tested up to 2 weeks. Nonetheless, it would have been interesting to assess the cross-reactivity of the sensor in the presence of dopamine, which has a similar oxidation potential as AA, as well as other potential analogues.

Diltemiz and Demirel have developed a quartz crystal microbalance (QCM) chip with embedded composite electrospun nanofibers bearing MIP NPs imprinted for the contaminant *p*-nitrophenol.<sup>[48b]</sup> The calculated LOD of the sensor was  $0.395 \text{ nM}$ , but although this is one of the first promising approaches at the integration of MIP electrospun sensors with QCM, further testing and optimization are required to assess the large-scale feasibility and the solidity of the approach.

Yang et al.<sup>[29d]</sup> developed the first integration of MIP electrospun materials with a photoelectrochemical detection method for triphenyl phosphate (TPhP), a typical model of organophosphorus flame retardants (OPFRs), which have been recently regarded as emerging environmental contaminants of health concern (Figure 7). Under the optimized experimental conditions, the photoelectrochemical response was linearly proportional to the logarithm value of TPhP concentrations in the range of  $0.01\text{--}500 \text{ ng mL}^{-1}$ , with an LOD of  $0.008 \text{ ng mL}^{-1}$ . Meanwhile, the sensor exhibited astonishingly high selectivity and stability, even after storage (1 month). This is an extremely interesting development in sensing applications for OPFRs, considering that the current analytical standards exhibit higher or comparable LODs, but they are also more expensive and time consuming.

#### 4.4. Biological and Therapeutic Applications

A first example of potential therapeutic applications of MIP electrospun nanofibers was formulated by Wu et al., who hypothesized the possibility of exploiting a PES electrospun

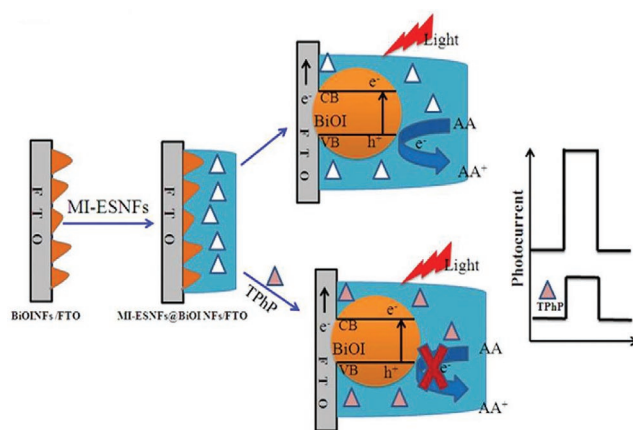


**Figure 7.** The principle of photoelectrochemical determination of TPhP using molecularly imprinted electrospun nanofibers (MI-ESNFs) produced on BiOI nanoflake arrays (BiOINFs) on fluorine-doped tin oxide glass (FTO). Reproduced with permission.<sup>[29d]</sup> Copyright 2017, Elsevier.

nanofiber mat as supporting material for a polydopamine bilirubin-imprinted MIP layer aimed at hemoperfusion in case of hyperbilirubinemia (Figure 8).<sup>[38]</sup>

Although the fiber mats were extremely blood biocompatible (did not exhibit significant hemolysis nor coagulation activity), the imprinting factor was not impressive (1.4), nor were the selectivity parameters for the structural analogues testosterone and cholesterol (1.43 and 1.11, respectively). Perhaps changing the MIP layer to a more selective or carefully designed polymer might improve the recognition performance for actual therapeutic applications.

With the aim of building a composite drug-delivery system for the sustained release of the anti-inflammatory drug dexamethasone, which currently exhibits a half-life of 2–5 h, Zahedi et al.<sup>[48i]</sup> have produced MIP NPs composite PCL electrospun nanofibers using methacrylic acid as functional monomer. The composite MIP nanofibers exhibited a sustained release of the drug (61% total over 4 days, with limited burst effect), in comparison to non-imprinted composite and plain PCL nanofibers, in which 70% and 85% of the drug were released within 24 h, respectively. Although a significant proportion of the drug remains trapped within the MIP matrix, the concentrations achieved are suitable for therapy. By optimizing the porosity of the composite system, perhaps, it could be possible to achieve an even higher release, thus further prolonging the therapeutic coverage with a single administration. This certainly represents a nice example for a preliminary potential therapeutic application, although it might have benefitted from the provision of both *in vitro* and *in vivo* data to assess also the biocompatibility and anti-inflammatory effect of the produced drug-delivery system.

Perhaps the first example of MIP electrospun fibers for regenerative medicine applications has been recently reported by Criscenti et al.,<sup>[44]</sup> who fabricated a bioactive scaffold (SMIES) for tissue regeneration. Currently, several techniques have been developed to modify the surface of scaffolds. Each of these approaches, however, exhibits some disadvantages, including poor controllability (coating), alteration of the bulk properties (blending, and wet chemical methods), and limited shelf-life (plasma treatment). In this work, the authors used PLGA

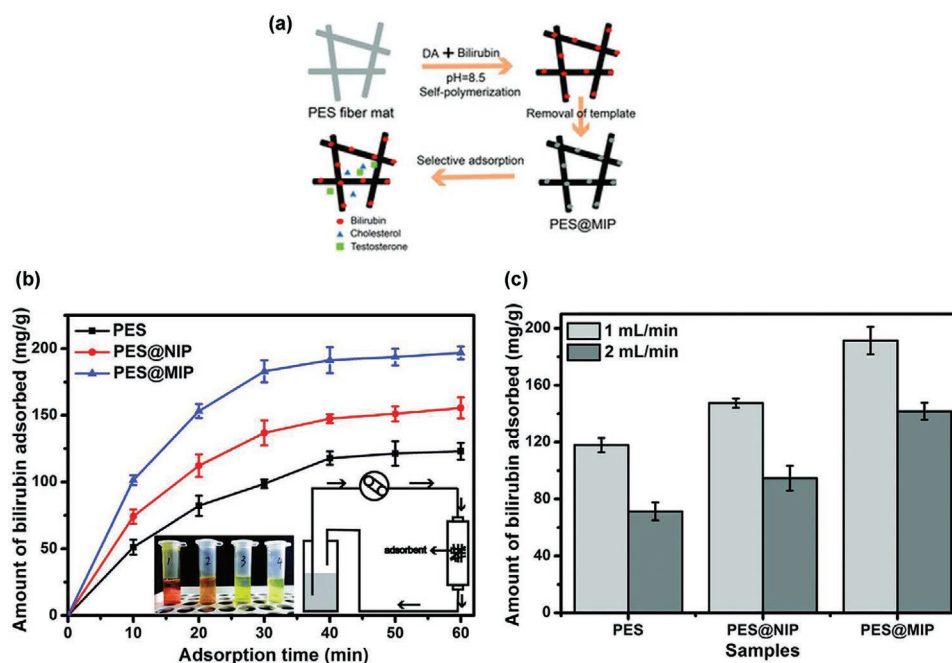


**Figure 8.** Production scheme and performance of the MIP nanofibers used in the work of Wu et al. A PES electrospun nanofiber mat was used as supporting material to produce a polydopamine bilirubin-imprinted MIP layer via the spontaneous polymerization of dopamine in a) weak alkaline conditions. The effect of b) the dialysis time and c) the flow rate on adsorption capacity of bilirubin on PES MIP nanofibers. Adapted with permission.<sup>[38]</sup> Copyright 2017, Royal Society of Chemistry.

imprinted with fluorescein isothiocyanate (FITC)-albumin, tetramethylrhodamine isothiocyanate (TRITC)-lectin, basic fibroblast growth factor (FGF-2), transforming growth factor beta 3 (TGF- $\beta$ 3) or bone morphogenetic protein 2 (BMP-2). The MIP PLGA scaffold showed mechanical and viscoelastic properties that matched the ones of native soft tissues, specifically ligament soft tissue. This is a particularly important aspect, since comparable mechanical properties between the native tissue and the synthetic substitute can promote adequate mechanical stimuli that contribute to cell growth and differentiation. Most importantly, the scaffolds bound selectively to each of the different proteins used, although for the two growth factors (GFs) the imprinting effect was much lower than for the other proteins, perhaps indicating that a better selection of the MIP matrix should be achieved. Nonetheless, the imprinting of GFs resulted in a significant effect on cell behavior: FGF-2 imprinted SMIES promoted cell proliferation and metabolic activity, while BMP-2 and TGF- $\beta$ 3 imprinted SMIES promoted cellular differentiation. Although these materials are extremely promising to steer endogenous tissue regeneration, as the authors correctly highlighted, their efficacy should be further evaluated in animals to compare and validate the results obtained *in vitro*.

## 5. Conclusion and Future Directions

This progress report comprehensively focuses on the production aspects and technological challenges as well as state-of-the-art applications of molecularly imprinted electrospun products. Molecular imprinting and electrospinning are undoubtedly of huge technological interest on their own, and according to

the reports analyzed in this report, the conjugation of these technologies indeed deserves attention for the design and development of smart and functional nanomaterials.

Despite the unique advantages deriving by producing MIPs via electrospinning for a plethora of applications, it is not surprising that this research avenue currently remains poorly explored. The processing challenges and optimization of parameters required to generate a nanomaterial that adequately satisfies all the expectations for both technologies are indeed difficult, as highlighted in the analysis of the production methods. Nonetheless, given the most recent developments on solid-phase MIP synthesis as well as MIP NPs integration, we would envisage that many more hybrid electrospun-MIP nanofibers will be developed in the coming years. The range of applications for which these composite materials can be used has been amply demonstrated, spanning from drug delivery, sensing/diagnostics, separation/filtration, bioremediation and waste removal, all the way up to tissue engineering and regenerative medicine.

Furthermore, we would expect that the conjugation of the two technologies will actually accelerate the commercial exploitation of MIPs. Indeed, so far the commercialization of MIP products has been extremely slow, with most of the examples involving the development of materials for separation (MIP Technologies, Polyintell, Semorex, Biotage/Sigma-Aldrich) or diagnostics (MIP Diagnostics Ltd.).

On the other hand, there are many electrospun-based commercial products available on the market, since 1995.<sup>[56]</sup> Currently, electrospun nanofibers are manufactured in large volumes by a number of companies, for use in healthcare (water/air filtration), automotive industry (oil filters, carbon emission reduction), medicine as drug delivery and tissue

engineering. Recently, Conformité Européene (CE) mark was awarded to the AVflo vascular access graft, which is based on electrospun products.<sup>[3a]</sup>

According to a recent report, the global nanofibers market size was estimated at USD 477.7 million in 2016 and is expected to register a compound annual growth rate of around 26% during 2019–2024.<sup>[57]</sup> According to these data, it appears as if there currently is an unexplored window of opportunity for MIP electrospun nanofibers, which deserves to be exploited. Starting from the examples discussed here, possible solution strategies can be envisaged to overcome the challenges for integrating MIPs and electrospinning, thus generating a library of new commercially exploitable MIP hybrid nanomaterials for next-level applications.

## Acknowledgements

The authors would like to acknowledge the National Research Foundation (NRF), Republic of Korea, for providing support through the Global Research Development Center Program (NRF-2018K1A4A3A01064257 and NRF-2018R1D1A1B07048020).

## Conflict of Interest

The authors declare no conflict of interest.

## Keywords

electrospinning, electrospay, molecular imprinting, molecularly imprinted polymers, nanotechnology

Received: March 1, 2020

Revised: April 21, 2020

Published online:

- [1] a) M. Thiruvengadam, G. Rajakumar, I.-M. Chung, *3 Biotech* **2018**, *8*, 74; b) N. Mitter, K. Hussey, *Nat. Nanotechnol.* **2019**, *14*, 508; c) A. P. Ramos, M. A. E. Cruz, C. B. Tovani, P. Ciancaglini, *Biophys. Rev.* **2017**, *9*, 79; d) J. R. Heath, *Proc. Natl. Acad. Sci. USA* **2015**, *112*, 14436.
- [2] T. Jiang, E. J. Carbone, K. W. H. Lo, C. T. Laurencin, *Prog. Polym. Sci.* **2015**, *46*, 1.
- [3] a) J. Xue, T. Wu, Y. Dai, Y. Xia, *Chem. Rev.* **2019**, *119*, 5298; b) R. S. Barhate, S. Ramakrishna, *J. Membr. Sci.* **2007**, *296*, 1; c) W. H. Carothers, Alkylene Ester of Polybasic Acids, *US Patent US2012267A*, **1935**; d) W. H. Carothers, Linear Condensation Polymers, *US Patent US2071250A*, **1937**.
- [4] Z.-M. Huang, Y. Z. Zhang, M. Kotaki, S. Ramakrishna, *Compos. Sci. Technol.* **2003**, *63*, 2223.
- [5] M. Mirjalili, S. Zohoori, *J. Nanostruct. Chem.* **2016**, *6*, 207.
- [6] a) F. Yang, R. Murugan, S. Wang, S. Ramakrishna, *Biomaterials* **2005**, *26*, 2603; b) R. Sridhar, R. Lakshminarayanan, K. Madhaiyan, V. Amutha Barathi, K. H. C. Lim, S. Ramakrishna, *Chem. Soc. Rev.* **2015**, *44*, 790; c) E. Ewaldz, R. Patel, M. Banerjee, B. K. Brettmann, *Polymer* **2018**, *153*, 529.
- [7] S. N. Reznik, A. L. Yarin, A. Theron, E. Zussman, *J. Fluid Mech.* **2004**, *516*, 349.
- [8] J. Doshi, D. H. Reneker, *J. Electrostat.* **1995**, *35*, 151.
- [9] F. Ding, H. Deng, Y. Du, X. Shi, Q. Wang, *Nanoscale* **2014**, *6*, 9477.
- [10] a) L. Chen, S. Xu, J. Li, *Chem. Soc. Rev.* **2011**, *40*, 2922; b) J. J. BelBruno, *Chem. Rev.* **2019**, *119*, 94.
- [11] a) C. Alexander, H. S. Andersson, L. I. Andersson, R. J. Ansell, N. Kirsch, I. A. Nicholls, J. O'Mahony, M. J. Whitcombe, *J. Mol. Recognit.* **2006**, *19*, 106; b) M. J. Whitcombe, N. Kirsch, I. A. Nicholls, *J. Mol. Recognit.* **2014**, *27*, 297; c) J. Fu, L. Chen, J. Lia, Z. Zhang, *J. Mater. Chem. A* **2015**, *3*, 13598; d) C. Branger, W. Meouche, A. Margaillan, *React. Funct. Polym.* **2013**, *73*, 859.
- [12] a) A. Poma, A. Guerreiro, S. Caygill, E. Moczko, S. Piletsky, *RSC Adv.* **2014**, *4*, 4203; b) H. Nishino, C.-S. Huang, K. J. Shea, *Angew. Chem., Int. Ed.* **2006**, *45*, 2392; c) R. Mahajan, M. Rouhi, S. Shinde, T. Bedwell, A. Incel, L. Mavliutova, S. Piletsky, I. A. Nicholls, B. Sellergren, *Angew. Chem., Int. Ed.* **2019**, *58*, 727; d) M. Dąbrowski, A. Zimińska, J. Kalecki, M. Cieplak, W. Lisowski, R. Maksym, S. Shao, F. D'Souza, A. Kuhn, P. S. Sharma, *ACS Appl. Mater. Interfaces* **2019**, *11*, 9265.
- [13] A. Poma, M. Whitcombe, S. Piletsky, in *Designing Receptors for the Next Generation of Biosensors*, Springer, Berlin **2012**, p. 105.
- [14] a) D. Gao, D.-D. Wang, Q. Zhang, F.-Q. Yang, Z.-N. Xia, Q.-H. Zhang, C.-S. Yuan, *J. Agric. Food Chem.* **2017**, *65*, 1158; b) R. I. Boysen, *J. Sep. Sci.* **2019**, *42*, 51; c) W. J. Cheong, S. H. Yang, F. Ali, *J. Sep. Sci.* **2013**, *36*, 609.
- [15] a) S. Piletsky, F. Canfarotta, A. Poma, A. M. Bossi, S. Piletsky, *Trends Biotechnol.* **2020**, *38*, 368; b) T. S. Bedwell, N. Anjum, Y. Ma, J. Czulak, A. Poma, E. Piletska, M. J. Whitcombe, S. A. Piletsky, *RSC Adv.* **2019**, *9*, 27849; c) H. Brahmabhatt, A. Poma, H. M. Pendergraft, J. K. Watts, N. W. Turner, *Biomater. Sci.* **2016**, *4*, 281; d) A. Poma, H. Brahmabhatt, J. K. Watts, N. W. Turner, *Macromolecules* **2014**, *47*, 6322; e) Z. Iskierko, P. S. Sharma, K. Bartold, A. Pietrzyk-Le, K. Noworyta, W. Kutner, *Biotechnol. Adv.* **2016**, *34*, 30; f) K. J. Jetzschmann, A. Yarman, L. Rustam, P. Kielb, V. B. Urlacher, A. Fischer, I. M. Weidinger, U. Wollenberger, F. W. Scheller, *Colloids Surf., B* **2018**, *164*, 240.
- [16] J. Fu, L. Chen, J. Li, Z. Zhang, *J. Mater. Chem. A* **2015**, *3*, 13598.
- [17] a) F. Canfarotta, L. Lezina, A. Guerreiro, J. Czulak, A. Petukhov, A. Daks, K. Smolinska-Kempisty, A. Poma, S. Piletsky, N. A. Barlev, *Nano Lett.* **2018**, *18*, 4641; b) S. A. Zaidi, *RSC Adv.* **2016**, *6*, 88807.
- [18] a) C. Malitesta, E. Mazzotta, R. A. Picca, A. Poma, I. Chianella, S. A. Piletsky, *Anal. Bioanal. Chem.* **2012**, *402*, 1827; b) L. Chen, X. Wang, W. Lu, X. Wu, J. Li, *Chem. Soc. Rev.* **2016**, *45*, 2137; c) M. Cieplak, W. Kutner, *Trends Biotechnol.* **2016**, *34*, 922; d) S. Wang, D. Yin, W. Wang, X. Shen, J. J. Zhu, H. Y. Chen, Z. Liu, *Sci. Rep.* **2016**, *6*, 22757.
- [19] a) S. Chigome, G. Darko, N. Torto, *Analyst* **2011**, *136*, 2879; b) S. Chigome, N. Torto, *Anal. Chim. Acta* **2011**, *706*, 25; c) I. S. Chronakis, L. Ye, in *Molecular Imprinting – Principles and Applications of Micro- and Nanostructure Polymers* (Ed: L. Ye), Jenny Stanford Publishing, New York **2013**, Ch. 6; d) B. Ghorani, N. Tucker, M. Yoshikawa, *Food Res. Int.* **2015**, *78*, 448; e) S. A. Zaidi, *Anal. Methods* **2015**, *7*, 7406.
- [20] a) E. P. Magennis, F. Fernandez-Trillo, C. Sui, S. G. Spain, D. J. Bradshaw, D. Churchley, G. Mantovani, K. Winzer, C. Alexander, *Nat. Mater.* **2014**, *13*, 748; b) C. H. Lim, C. D. Ki, T. H. Kim, J. Y. Chang, *Macromolecules* **2004**, *37*, 6; c) A. Motib, A. Guerreiro, F. Al-Bayati, E. Piletska, I. Manzoor, S. Shafeeq, A. Kadam, O. Kuipers, L. Hiller, T. Cowen, S. Piletsky, P. W. Andrew, H. Yesilkaya, *Angew. Chem., Int. Ed.* **2017**, *56*, 16555; d) A. Cutivet, C. Schembri, J. Kovensky, K. Haupt, *J. Am. Chem. Soc.* **2009**, *131*, 14699; e) J. L. Liao, Y. Wang, S. Hjertén, *Chromatographia* **1996**, *42*, 259.
- [21] a) K. N. Awokoya, B. A. Moronkola, S. Chigome, D. A. Ondigo, Z. Tshentu, N. Torto, *J. Polym. Res.* **2013**, *20*, 148; b) K. N. Awokoya, Z. Tshentu, N. Torto, *Afr. J. Pure Appl. Chem.* **2015**, *9*, 223.
- [22] a) I. S. Chronakis, B. Milosevic, A. Frenot, L. Ye, *Macromolecules* **2006**, *39*, 357; b) M. Yoshikawa, K. Nakai, H. Matsumoto,

- A. Tanioka, M. D. Guiver, G. P. Robertson, *Macromol. Rapid Commun.* **2007**, 28, 2100; c) W. J. Kim, J. Y. Chang, *Mater. Lett.* **2011**, 65, 1388.
- [23] X. Xue, R. Lu, Y. Li, Q. Wang, J. Li, L. Wang, *Analyst* **2018**, 143, 3465.
- [24] F. Ruggieri, A. A. D'Archivio, D. Di Camillo, L. Lozzi, M. A. Maggi, R. Mercurio, S. Santucci, *J. Sep. Sci.* **2015**, 38, 1402.
- [25] A. Betatache, M. Braiek, J. F. Chateaux, F. Lagarde, N. Jaffrezic-Renault, *Key Eng. Mater.* **2013**, 543, 84.
- [26] Y. Sueyoshi, A. Utsunomiya, M. Yoshikawa, G. P. Robertson, M. D. Guiver, *J. Membr. Sci.* **2012**, 401–402, 89.
- [27] Y. Sueyoshi, C. Fukushima, M. Yoshikawa, *J. Membr. Sci.* **2010**, 357, 90.
- [28] M. Yoshikawa, J. Isezaki, *J. Membr. Sep. Technol.* **2014**, 3, 119.
- [29] a) L.-S. Wan, J. Wu, Z.-K. Xu, *Macromol. Rapid Commun.* **2006**, 27, 1533; b) Z. Wei, Q. Zhang, L. Wang, M. Peng, X. Wang, S. long, J. Yang, *J. Polym. Sci., Part B: Polym. Phys.* **2012**, 50, 1414; c) A. S. Ogunlaja, M. J. Coombes, N. Torto, Z. R. Tshentu, *React. Funct. Polym.* **2014**, 81, 61; d) X. Yang, X. Li, L. Zhang, J. Gong, *Biosens. Bioelectron.* **2017**, 92, 61.
- [30] a) R. Zhao, X. Li, B. Sun, Y. Li, Y. Li, C. Wang, *Chem. Res. Chin. Univ.* **2017**, 33, 986; b) X. Liu, J. I. Yang, L. y. Tong, Q. Zhang, X. w. Li, J. d. Chen, *Chem. Res. Chin. Univ.* **2015**, 31, 1062; c) P. M. Gore, L. Khurana, S. Siddique, A. Panicker, B. Kandasubramanian, *Environ. Sci. Pollut. Res.* **2018**, 25, 3320.
- [31] a) M. M. Moein, M. Javanbakht, M. Karimi, B. Akbari-adergani, *J. Sep. Sci.* **2015**, 38, 1372; b) M. M. Moein, M. Javanbakht, M. Karimi, B. Akbari-adergani, *Talanta* **2015**, 134, 340.
- [32] a) C. S. Ki, E. H. Gang, I. C. Um, Y. H. Park, *J. Membr. Sci.* **2007**, 302, 20; b) Y. Li, T. Qiu, X. Xu, *Eur. Polym. J.* **2013**, 49, 1487; c) Y. Li, C. Xu, T. Qiu, X. Xu, *J. Nanosci. Nanotechnol.* **2015**, 15, 4245; d) Y. Li, J. Zhang, C. Xu, Y. Zhou, *Sci. China: Chem.* **2016**, 59, 95; e) X. Ma, Z. Chen, X. Chen, R. Chen, X. Zheng, *Chin. J. Chem.* **2011**, 29, 1753.
- [33] Y. Zhang, Q. Wei, Q. Zhang, J. Li, J. Yang, C. Zhao, *Sep. Sci. Technol.* **2011**, 46, 1615.
- [34] A.-f. Che, Y.-f. Yang, L.-s. Wan, J. Wu, Z.-k. Xu, *Chem. Res. Chin. Univ.* **2006**, 22, 390.
- [35] a) B. Sellergren, B. Rückert, A. J. Hall, *Adv. Mater.* **2002**, 14, 1204; b) B. Rückert, A. J. Hall, B. Sellergren, *J. Mater. Chem.* **2002**, 12, 2275.
- [36] S. Minko, in *Polymer Surfaces and Interfaces: Characterization, Modification and Applications* (Ed: M. Stamm), Springer, Berlin **2008**, p. 215.
- [37] Y. Zhai, D. Wang, H. Liu, Y. Zeng, Z. Yin, L. Li, *Anal. Sci.* **2015**, 31, 793.
- [38] K. Wu, W. Yang, Y. Jiao, C. Zhou, *J. Mater. Chem. B* **2017**, 5, 5763.
- [39] C. J. Tan, Y. W. Tong, *Anal. Bioanal. Chem.* **2007**, 389, 369.
- [40] C. Sulitzky, B. Rückert, A. J. Hall, F. Lanza, K. Unger, B. Sellergren, *Macromolecules* **2002**, 35, 79.
- [41] B. Sellergren, A. J. Hall, in *Techniques and Instrumentation in Analytical Chemistry*, Vol. 23 (Ed: B. Sellergren), Elsevier, New York **2001**, p. 21.
- [42] a) E. Yilmaz, K. Haupt, K. Mosbach, *Angew. Chem., Int. Ed.* **2000**, 39, 2115; b) M. M. Titirici, B. Sellergren, *Anal. Bioanal. Chem.* **2004**, 378, 1913; c) L. Liu, J. Zheng, G. Fang, W. Xie, *Anal. Chim. Acta* **2012**, 726, 85; d) S. Subrahmanyam, A. Guerreiro, A. Poma, E. Moczko, E. Piletska, S. Piletsky, *Eur. Polym. J.* **2013**, 49, 100; e) A. Poma, A. Guerreiro, M. J. Whitcombe, E. V. Piletska, A. P. Turner, S. A. Piletsky, *Adv. Funct. Mater.* **2013**, 23, 2821; f) K. Muzyka, K. Karim, A. Guerreiro, A. Poma, S. Piletsky, *Nanoscale Res. Lett.* **2014**, 9, 154; g) F. Canfarotta, A. Poma, A. Guerreiro, S. Piletsky, *Nat. Protoc.* **2016**, 11, 443; h) H.-H. Yang, S.-Q. Zhang, F. Tan, Z.-X. Zhuang, X.-R. Wang, *J. Am. Chem. Soc.* **2005**, 127, 1378; i) X. Shen, L. Ye, *Macromolecules* **2011**, 44, 5631.
- [43] T. Zhu, D. Xu, Y. Wu, J. Li, M. Zhou, T. Tian, Y. Jiang, F. Li, G. Li, *J. Mater. Chem. B* **2013**, 1, 6449.
- [44] G. Criscenti, C. De Maria, A. Longoni, C. A. van Blitterswijk, H. A. M. Fernandes, G. Vozzi, L. Moroni, *Biofabrication* **2018**, 10, 045005.
- [45] J. Gaitzsch, M. Delahaye, A. Poma, F. Du Prez, G. Battaglia, *Polym. Chem.* **2016**, 7, 3046.
- [46] P. P. S. S. Abadi, J. C. Garbern, S. Behzadi, M. J. Hill, J. S. Tresback, T. Heydari, M. R. Eftehadi, N. Ahmed, E. Copley, H. Aghaverdi, R. T. Lee, O. C. Farokhzad, M. Mahmoudi, *Adv. Funct. Mater.* **2018**, 28, 1707378.
- [47] I. S. Chronakis, A. Jakob, B. Hagström, L. Ye, *Langmuir* **2006**, 22, 8960.
- [48] a) K. Yoshimatsu, L. Ye, J. Lindberg, I. S. Chronakis, *Biosens. Bioelectron.* **2008**, 23, 1208; b) K. Yoshimatsu, L. Ye, P. Stenlund, I. S. Chronakis, *Chem. Commun.* **2008**, 2022; c) S. Piperno, B. Tse Sum Bui, K. Haupt, L. A. Gheber, *Langmuir* **2011**, 27, 1547; d) H. Liu, X. Lei, Y. Zhai, L. Li, *Adv. Chem. Eng. Sci.* **2012**, 02, 266; e) L. Zhang, Y. Guo, W.-h. Chi, H.-g. Shi, H.-q. Ren, T.-y. Guo, *Chin. J. Polym. Sci.* **2014**, 32, 1469; f) F. Liu, Q. Liu, Y. Zhang, Y. Liu, Y. Wan, K. Gao, Y. Huang, W. Xia, H. Wang, Y. Shi, Z. Huang, B. Lu, *Chem. Eng. J.* **2015**, 262, 989; g) Y.-t. Wu, Y.-h. Zhang, M. Zhang, F. Liu, Y.-c. Wan, Z. Huang, L. Ye, Q. Zhou, Y. Shi, B. Lu, *Food Chem.* **2014**, 164, 527; h) S. Diltemiz, R. Demirel, *EIJST* **2016**, 5, 47; i) P. Zahedi, M. Fallah-Darrehchi, S. A. Nadoushan, R. Aeinehvand, L. Bagheri, M. Najafi, *Korean J. Chem. Eng.* **2017**, 34, 2110; j) M. Hassanzadeh, M. Ghaemy, S. M. Amininasab, Z. Shami, *React. Funct. Polym.* **2018**, 130, 70; k) M. Demirkurt, Y. A. Olcer, M. M. Demir, A. E. Eroglu, *Anal. Chim. Acta* **2018**, 1014, 1.
- [49] R. Büttiker, J. Ebert, C. Hinderling, C. Adlhart, *CHIMIA Int. J. Chem.* **2011**, 65, 182.
- [50] P. Tonglairoum, W. Chaijaroenluk, T. Rojanarata, T. Ngawhirunpat, P. Akkaramongkolporn, P. Opanasopit, *AAPS PharmSciTech* **2013**, 14, 838.
- [51] A. Poma, A. P. Turner, S. A. Piletsky, *Trends Biotechnol.* **2010**, 28, 629.
- [52] M. Rammika, G. Darko, N. Torto, *Water SA* **2011**, 37, 539.
- [53] M. Yoshikawa, A. Tanioka, H. Matsumoto, *Curr. Opin. Chem. Eng.* **2011**, 1, 18.
- [54] H. Dai, L. Gong, G. Xu, X. Li, S. Zhang, Y. Lin, B. Zeng, C. Yang, G. Chen, *Analyst* **2015**, 140, 582.
- [55] S. Wei, Y. Zhang, M. Zhou, *Sens. Rev.* **2014**, 34, 327.
- [56] D. H. Reneker, I. Chun, *Nanotechnology* **1996**, 7, 216.
- [57] ResearchAndMarkets.com, Globe Newswire **2019**, <https://www.researchandmarkets.com/reports/4514872/nanofiber> (Accessed: December 2019).